Inorg. Chem. **2007**, *46*, 10624–10631

Direct Atomic Scale Observation of Linkage Isomerization of As_4S_4 Clusters during the Photoinduced Transition of Realgar to Pararealgar†

Panče Naumov,*,‡,§,|| Petre Makreski,|| and Gligor Jovanovski||,⊥

Frontier Research Base for Global Young Researchers, Graduate School of Engineering, Osaka University, 2-1 Yamadaoka, Suita 565-0871, Osaka, Japan, National Institute for Materials Science, ICYS, 1-1 Namiki, Tsukuba, Ibaraki 305-0044, Japan, Institute of Chemistry, Faculty of Science, Sts Cyril and Methodius University, P.O. Box 162, MK-1001 Skopje, Macedonia, and Macedonian Academy of Sciences and Arts, P.O. Box 428, MK-1001 Skopje, Macedonia

Received July 2, 2007

The reaction mechanism underlying the photoinduced linkage isomerization of discrete arsenic–sulfur clusters in the realgar form of tetraarsenic tetrasulfide (α-As_4S_4) to its pararealgar form was studied on a natural specimen of the mineral with a combination of in situ single-crystal X-ray photodiffraction and Fourier transform infrared spectroscopy. The photodiffraction technique provided direct atomic resolution evidence of formation of intermediate As_4S_5 phase in which half of the realgar molecule is retained in its envelope-type conformation, while the other half is transformed by effective switching of positions of one sulfur and one arsenic atom. The initiation and propagation stages of the process are studied under light and dark conditions, during and after photoexcitation with polychromatic visible light. In the "light" reaction stage, the interatomic and cell parameters averaged over the crystal volume and photoexcitation time remain almost unchanged. The residual electron density features are indicative for formation of a small amount of As_4S_5 clusters, which at this stage do not affect the overall crystalline order. In the "dark" reaction stage, a set of self-sustainable autocatalytic reactions results in strong and nearly isotropic expansion of the unit cell. The structure in the dark stage represents direct evidence of formation of pararealgar which was obtained in yield of about 5% in the single crystal of realgar. The cell expansion is due to increased mole ratio of clusters of pararealgar relative to realgar and to increased intercluster separation. Due to lattice incompatibility, a higher content of the product results in progressive decrease of crystal quality. Creation of small amount of arsenolite (As_2O_3) which appears as byproduct in the light stage and remains unreacted in the product mixture was confirmed by far-IR spectroscopy.

1. Introduction

Due to their photochemical sensitivity, arsenic chalcogenides are important materials for use in optics, as lithography photoresists, in optical memories and switches, in modulators, in media for optical computing, and as pn junctions.[1−3] Thin films of arsenic sulfides have been recently considered as materials for optical fibers.[4,5] Large number of arsenic sulfide clusters of various sizes and compositions can be obtained by pulsed laser ablation.[6] Probably the best studied arsenic sulfides are arsenic(III) sulfide, As_2S_3, also known as the mineral orpiment, and the low-temperature stable α modification of arsenic(II) sulfide, α-As_4S_4, which as the mineral realgar occurs in the nature in the form of red to orange prismatic striated crystals, grains, crusts, and

† Dedicated to Academician Bojan Šoptrajanov, the leader of the Molecular Spectroscopy Group in Macedonia, on the occasion of his 70th birthday.

* To whom correspondence should be addressed at the Graduate School of Engineering, Osaka University, 2-1 Yamadaoka, Suita 565-0871, Osaka, Japan. E-mail: npance@wakate.frc.eng.osaka-u.ac.jp, npance@hotmail.com.
‡ Osaka University, 2-1 Yamadaoka, Suita 565-0871, Osaka, Japan
§ National Institute for Materials Science.
|| Sts Cyril and Methodius University.
⊥ Macedonian Academy of Sciences and Arts.

(1) Chern, G. C.; Lauks, I. *J. Appl. Phys.* **1982**, *53*, 6979−6982.
(2) De Neufville, J. P.; Moss, S. C.; Ovshinski, S. R. *J. Non-Cryst. Solids* **1973**, *13*, 191−223.
(3) Kolobov, A. V. *J. Non-Cryst. Solids* **1993**, *166*, 1159−1164.
(4) Kobelke, J.; Jetschke, S.; Schwuchow, A.; Kirchof, J.; Schuster, K. *J. Non-Cryst. Solids* **2003**, *326/327*, 446−450.
(5) Nguyen, V. Q.; Sanghera, J. S.; Cole, B.; Pureza, P.; Kung, F. H.; Aggarwal, I. D. *J. Am. Ceram. Soc.* **2002**, *85*, 2056−2058.
(6) Spalt, Z.; Alberti, M.; Pena-Mendez, E.; Havel, J. *Polyhedron* **2005**, *24*, 1417−1424.

10.1021/ic701299w CCC: $37.00
Published on Web 11/10/2007

earthy masses.[7−10] α-As_4S_4 is stable up to about 513 K where it undergoes structural transition to the high-temperature β form, β-As_4S_4. The transition temperature is impurity-dependent, ranging between 513 and 538 K in the presence of elemental As and orpiment, respectively.[7,11] The β form can be also prepared by direct synthesis at 525 K.[11] Two synthetic phases, As_4S_4(II)[12] and γ-As_4S_4,[7,11] have been also reported. Roberts et al.[13] were the first to clarify that the yellow film usually covering the surface of realgar, which in the past had been confused with the mineral orpiment, is a distinct phase termed pararelagar. Douglass et al.[14] produced pararealgar as a yellow-orange powder by exposure of realgar to sunlight or artificial visible light (500−670 nm). Pararealgar was later crystallographically authenticated by Bonazzi et al.[15] Although infrared[16−23] and Raman[17,24,25] spectra of realgar have been well studied and the Raman spectrum of pararealgar has been described in several reports,[26,27] to the best of our knowledge, the infrared spectrum of pararealgar has not been reported yet. The structures of realgar, pararealgar, tetraarsenic trisulfide, and tetraarsenic pentasulfide consist of discrete arsenic−sulfur clusters, whereas the structure of orpiment is polymeric (Figure 1). The packing of the discrete cages of realgar and pararealgar in the respective lattices is also different (Figure 2).

The photoinduced transition of realgar to pararealgar was monitored with Raman spectroscopy,[26,27] and the change of lattice parameters was studied with X-ray diffraction (XRD).[27−29] The transformation includes an intermediate−expanded β phase, which was initially termed χ phase, and arsenolite (As_2O_3) as a minor side product. Several reaction mechanisms have been suggested, but a consensus on all details of the reaction mechanism has not been reached yet. According to the most recent model, initially suggested by

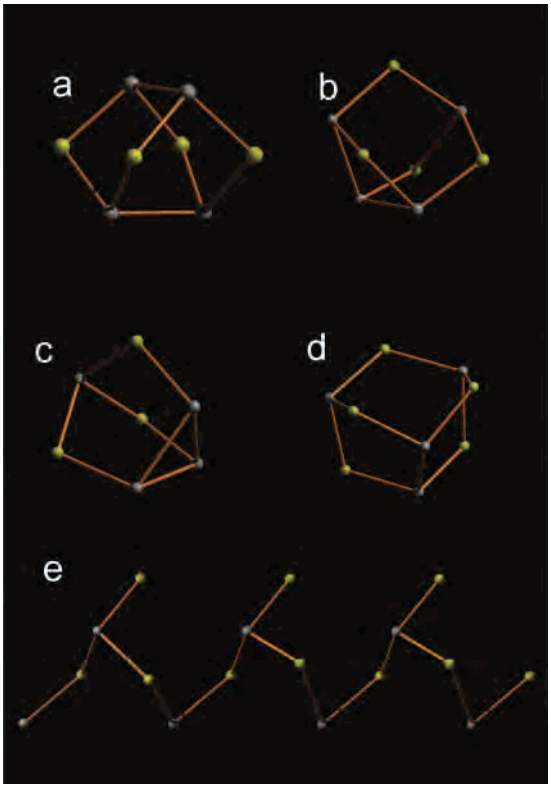

Figure 1. Arsenic−sulfur clusters in the structures of realgar (As_4S_4, a), pararealgar (As_4S_4, b), tetraarsenic trisulfide (As_4S_3, c), and tetraarsenic pentasulfide (As_4S_5, d). Part of the polymeric layered structure of orpiment, As_2S_3 (e), is shown for comparison. The arsenic and sulfur atoms are represented as gray and yellow circles, respectively.

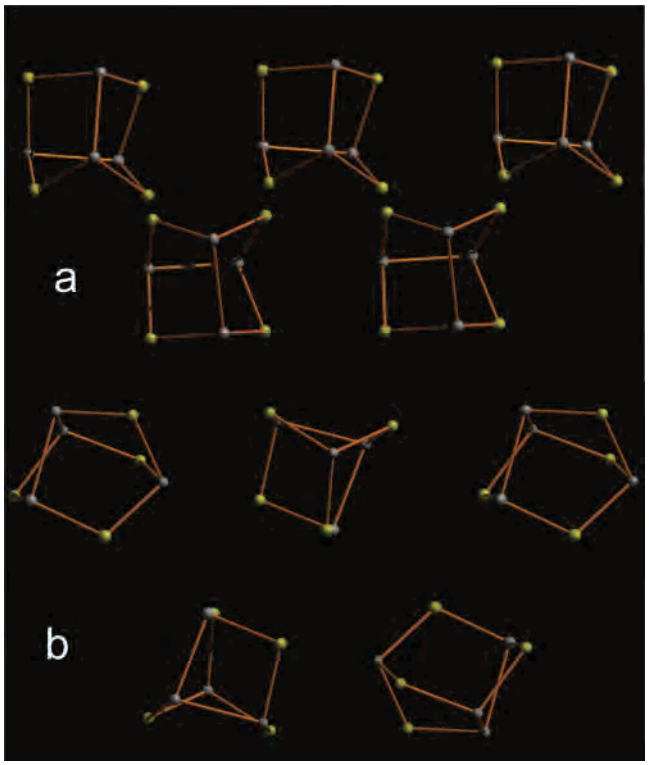

Figure 2. Molecular packing in the structures of realgar (a) and pararealgar (b). The arsenic and sulfur atoms are represented as gray and yellow circles, respectively.

(7) Hall, H. T. Ph.D. Thesis, Brown University, Providence, RI, 1966.
(8) Clark, A. H. *Am. Mineral.* **1970**, *55*, 1338−1344.
(9) Mullen, D. J. E.; Nowacki, W. *Z. Kristallogr.* **1972**, *136*, 48−65.
(10) Ito, T.; Morimoto, N.; Sadanaga, R. *Acta Crystallogr.* **1952**, *5*, 775−782.
(11) Roland, G. W. *Can. Mineral.* **1972**, *11*, 520−525.
(12) Kutoglu, A. *Z. Anorg. Allg. Chem.* **1976**, *419*, 176−184.
(13) Roberts, A. C.; Ansell, H. G.; Bonardi, M. *Can. Mineral.* **1980**, *18*, 525−527.
(14) Douglass, D. L.; Shing, C. C.; Wang, G. *Am. Mineral.* **1992**, *77*, 1266−1274.
(15) Bonazzi, P.; Menchetti, S.; Pratesi, G. *Am. Mineral.* **1995**, *80*, 400−403.
(16) Billes, F.; Mitsa, V.; Fejes, I.; Mateleshko, N.; Fejsa, I. *J. Mol. Struct.* **1999**, *513*, 109−115.
(17) Forneris, R. *Am. Mineral.* **1969**, *54*, 1062−1074.
(18) Šoptrajanov, B.; Trajkovska, M.; Jovanovski, G.; Stafilov, T. *Neues Jahrb. Mineral. Abh.* **1994**, *167*, 329−337.
(19) Soong, R.; Farmer, V. C. *Mineral. Mag.* **1978**, *42*, M17−M20.
(20) Muniz-Miranda, M.; Sbrana, G.; Bonazzi, P.; Menchetti, S.; Pratesi, G. *Spectrochim. Acta* **1996**, *24*A, 1391−1401.
(21) Banerjee, A.; Jensen, J. O.; Jensen, J. L. *J. Mol. Struct.* **2003**, *626*, 63−75.
(22) Mori, T.; Matsuishi, K.; Arai, T. *J. Non-Cryst. Solids* **1984**, *65*, 269−283.
(23) Bues, W.; Somer, M.; Brockner, W. *Z. Anorg. Allg. Chem.* **1983**, *499*, 7−14.
(24) Scheuermann, W.; Ritter, G. J. *Z. Naturforsch.* **1969**, *24A*, 408−411.
(25) Frost, R. L.; Martens, W. N.; Kloprogge, J. T. *Neues Jahrb. Mineral. Monatsh.* **2002**, *10*, 469−480.
(26) Trentelman, K.; Stodulski, L.; Pavlosky, M. *Anal. Chem.* **1996**, *68*, 1755−1761.
(27) Bonazzi, P.; Menchetti, S.; Pratesi, G.; Muniz-Miranda, M.; Sbrana, G. *Am. Mineral.* **1996**, *81*, 874−880.
(28) Ballirano, P.; Maras, A. *Eur. J. Mineral.* **2006**, *18*, 589−599.
(29) Kyono, A.; Kimata, M.; Hatta, T. *Am. Mineral.* **2005**, *90*, 1563−1570.

Bonazzi et al.[30] and later supported by the results of Kyono et al.,[29] the initiating photoreaction step requires oxygen and can be represented as

$$5As_4S_4 + 3O_2 \rightarrow 4As_4S_5 + 2As_2O_3 \quad (1)$$

$$As_4S_5 \rightarrow As_4S_4 + S \quad (2)$$

The process continues through a set of cyclic reactions in which the sulfur atom released by the decomposition of As_4S_5 (eq 2) reacts with a molecule of realgar to produce a molecule of pararealgar, whereupon a sulfur atom is released which continues the process (eqs 3 and 4):

$$S + As_4S_{4(realgar)} \rightarrow As_4S_5 \quad (3)$$

$$As_4S_5 \rightarrow As_4S_{4(pararealgar)} + S \quad (4)$$

According to the previous studies,[27,29] the transition proceeds by linear increase of the unit cell volume of about 10 Å^3, caused by anisotropic expansion of the cell along the *a* and *c* axes. The cell expansion is related to formation of the χ phase,[14] which was supposed to exist as less-ordered form of the high-temperature modification β-As_4S_4. The Raman spectra identified the χ phase as orange material giving rise to a strong peak at 360 cm^{-1}.[20,26] Powder XRD data based on a quaternary phase model of the reaction (realgar, pararealgar, χ phase, arsenolite) suggested that the composition of the intermediate phase is close to $As_4S_{4.2}$.[28] The recent detailed diffraction studies by Bonazzi et al.[31,32] of light-induced transformation of solid solutions of intermediate compositions between β-As_4S_4 and As_8As_9 (the latter is known as the mineral alacranite, composed of equal amounts of As_4S_4 and As_4S_5 cages) identified the intermediate χ phase as β-As_4S_4. On the basis of comparison with a series of mixed crystals As_8S_{9-x} exhibiting a linear increase of cell volume with the As_4S_5/As_4S_4 ratio,[30] it was suggested that the light-induced cell expansion of realgar is caused by formation of As_4S_5 molecules.[30,33] This has been recently evidenced for the case of photoirradiated β-As_4S_4 and its solid solutions by single-crystal XRD.[32] The product As_4S_5 (naturally occurring as the mineral uzonite) is insensitive to light,[34] but in the lattice of realgar it spontaneously decays to pararealgar and atomic (radical) sulfur. On the other hand, Kyono et al.[29] prescribed the cell expansion of irradiated realgar to increase of distance between the As_4S_4 centroids, because according to the single-crystal XRD results the sphericity and volume of the As_4S_4 cages remain practically constant. Along with the proposed mechanism (eqs 1−4), powder XRD study[28] of partially transformed realgar showed presence, besides pararealgar, of arsenolite and an intermediate phase along the β-As_4S_4-alacranite series, with overall approximate composition of As_4S_{4+x} ($0.18 < x < 0.25$). The formation of arsenolite as colorless or white side product has been confirmed by XPS and Raman microspectroscopy,[29] and possible formation of sulfur oxides was also postulated.[28]

Although the mechanism of light-induced transformation of the high-temperature phase β-As_4S_4 and of its mixed crystals has been recently unraveled,[31,32] no direct evidence of the reaction in the case of realgar at atomic level has been reported yet. Particularly, no evidence of additional sulfur atoms or of the geometrical change supporting the hypothesized mechanism has been provided. It is also not clear whether the transformation proceeds through any well-defined additional intermediate phases. Here we report the first direct atomic level evidence for the mechanism of the photoinduced transformation of realgar, obtained with in situ single-crystal X-ray photodiffraction. The formation of the intermediate and product phases in a single crystal was directly observed. The results are aided by detailed in situ IR spectroscopic study of the process and identification of involved phases.

2. Experimental Section

A natural specimen of realgar was collected from the Allchar locality (Macedonia). For the spectroscopic measurements, well-formed red crystals measuring a few millimeters were separated from the ore and powdered. The transition was monitored by exposure of powdered realgar samples to natural sunlight during 30, 60, 90, 120, 150, and 180 days. In addition, a product rich with pararealgar was obtained by exposure of pure realgar to natural sunlight during almost 3 years (1000 days) to ensure complete conversion. The 500−150 cm^{-1} region of the far-IR spectra was recorded from Nujol-suspended samples at room temperature using a Perkin-Elmer FTIR 2000 interferometer. Curve fitting of the IR spectra was performed using mixed Gaussian−Lorentzian functions for the peak shape and linear function for the spectral baseline.

Single-crystal XRD data were collected in ω-oscillation mode with an APEX Bruker three-circle diffractometer equipped with CCD detector, using graphite-monochromatized Mo Kα X-ray radiation (0.71073 Å, 40 kV, 40 mA). In the case of crystals **A** and **B** (see below), 1900 and 1400 frames of 0.3° width were collected by exposure of 20 and 30 s/frame, respectively. The frames were collected with the SMART software and merged and integrated by using SAINT.[35] The set of reflections were further processed by XPREP and corrected for absorption with SADABS.[35] The structures were solved with direct methods[36] and refined on F^2,[37] assigning anisotropic displacement parameters to all atoms.

To prevent conversion induced by room light, all sample handling and data collection procedures were performed in the dark or under a red safe-light ($\lambda > 670$ nm). Because the photoreaction is irreversible, the alteration of crystal structure in the dark was studied on two different well-diffracting single crystals of realgar. Both single crystals were cut off from the interior of a large light-protected red crystalline block of the natural mineral, and they appeared red and transparent. For each crystal, X-ray diffraction

(30) Bonazzi, P.; Bindi, L.; Olmi, F.; Menchetti, S. *Eur. J. Mineral.* **2003**, *15*, 283−288.
(31) Bindi, L.; Bonazzi, P. *Am. Mineral.* **2007**, *92*, 617−620.
(32) Bonazzi, P.; Bindi, L.; Pratesi, G.; Menchetti, S. *Am. Mineral.* **2006**, *91*, 1323−1330.
(33) Ballirano, P.; Maras, A. *32nd International Geological Congress Program and Abstract*; 2004; p 489.
(34) Bindi, L.; Popova, V.; Bonazzi, P. *Can. Mineral.* **2003**, *41*, 1463−1468.
(35) *SAINT−Siemens Area Detector Integration and SMART−Siemens Molecular Analysis Research Tool*; Siemens Analytical X-ray Instruments Inc.: Madison, WI, 1996.
(36) Altomare, A.; Cascarano, G.; Giacovazzo, C.; Guagliardi, A.; Burla, M. C.; Polidori, G.; Camalli, M. *J. Appl. Crystallogr.* **1994**, *27*, 435−436.
(37) Sheldrick, G. M. E. *SHELXL-97. Structure refinement program*; University of Göttingen: Göttingen, Germany, 1997.

Table 1. Far-IR Active Band Frequencies (cm^{-1}) and Intensities of Realgar (α-As_4S_4)

this work[a]	Šoptrajanov et al.[18]	Muniz-Miranda et al.[20]	Soong and Farmer[19]	Farmer[38]
374 m	378	376	375	374
368 m	368	370	369	367
358 w	359	355	360	359
		345		
341 vs	341	341	341	341
327 sh		330		
225 s	224	222	226	224
210 w	210	212	210	210
203 w	202		204	204
193 w	192	196	194	193
183 w	183	184	183	183
		173		
168 m	166	167	170	169

[a] Intensity codes: vs, very strong; s, strong; w, weak; m, medium; sh, shoulder.

data were collected using an identical strategy for data collection before irradiation and after/during light irradiation. The light reaction stage of the transition was studied from a crystal of size 0.30 × 0.25 × 0.20 mm (crystal **A**). After a complete diffraction dataset was collected in the dark, a second dataset was collected during exposure (ca. 12.5 h) of crystal **A** to continuous polychromatic light from a 200 W mercury−halogen lamp (Supercure 203S model with C-type mirror, SAN-EI). It has been demonstrated[14] that only light in the 500−670 nm region of the spectrum is absorbed by realgar, while the remaining wavelengths practically do not interact with the sample. The end of the unfocused optical fiber guide output was fixed at about 2.5 cm from the sample mounted on the goniometer head. The light was kept at very low intensity (∼5%), and the chamber of the diffractometer was purged with nitrogen gas to decrease the heating. To study the dark reaction stage, the first dataset was collected in the dark from another crystal of size 0.22 × 0.20 × 0.10 mm (crystal **B**). The crystal was then irradiated with the same visible light source during the collection of reflections for unit cell determination (1.3 h). After the irradiation was stopped, a second set of X-ray diffraction data was collected in the dark from the irradiated crystal **B**.

3. Results and Discussion

3.1. Monitoring of the Transition with FT IR Spectroscopy. The far-IR spectrum of pure realgar at ambient temperature consists of two regions, As−S stretchings between 380 and 320 cm^{-1} and As−S−As bendings between 230 and 150 cm^{-1}, with the low-frequency As−As stretching[20] at 183 cm^{-1} (Tables 1 and 2). The spectrum recorded from our specimen conforms to the earlier reports of the spectrum of form a.[18−20,38] We observed a shoulder at 327 cm^{-1} reported by Muniz-Miranda et al.,[20] but similarly to other authors,[18,19,38] we could not detect a band at 345 cm^{-1}.[20]

Figure 3 presents the effect of exposure to sunlight on the far-IR spectrum of realgar. The weak bands evolving above 400 cm^{-1} after about 90 days are prescribed to arsenolite, since they strongly coincide with the corresponding bands in the IR spectrum of the pure mineral.[39] As expected from the decreased molecular symmetry and/or increased number of phases, the irradiation (below 400 cm^{-1}) results in notable

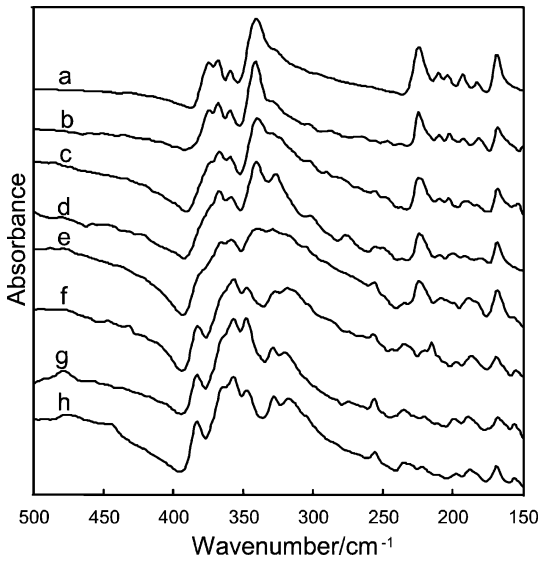

Figure 3. Effect of irradiation on the far-IR spectrum of realgar (a) exposed to natural sunlight under normal humidity conditions during 30 (b), 60 (c), 90 (d), 120 (e), 150 (f), 180 (g), and 1000 (h) days.

spectral changes, increased number and blue or red shift of the bands (Table 2). Upon exposure to light, the intensity of the band at 374 cm^{-1} decreases, disappearing completely after 90 days, and after 120 days a shoulder appears at 381 cm^{-1} (Figure 3). The intensities of the blue-shifted bands at 374 and 341 cm^{-1} decrease and the band at 358 cm^{-1} increases, whereas the shoulder at 327 cm^{-1} remains unaffected. After 30 days of irradiation, new bands at 256 and 236 cm^{-1} appear, and after 120 and 150 days, new bands at 156 and 319 cm^{-1} evolve. Contrary to the As−S stretchings, the bands in the low-frequency region (225−150 cm^{-1}) appear at the same positions or they are red-shifted in the spectrum of pararealgar. The intensity of the ω(As−S−As) mode[20] at 225 cm^{-1} is decreased, whereas the intensity of the band at 168 cm^{-1} prescribed to the same mode remains unaffected. The frequencies and intensities of the δ(As−S−As) (210 cm^{-1}) and ν(As−As) (183 cm^{-1}) modes also remain unaffected. The overall spectral change indicate that the band appearance in the 205−185 cm^{-1} region can be employed to distinguish among different As_4S_4 polymorphs.

3.2. Direct Observation of the Transition with Single-Crystal X-ray Photodiffraction. As it can be inferred from the suggested mechanism (eqs 1−4), the process of photoinduced transformation of realgar to pararealgar consists of two stages: "light" initiation stage, during which the photoreaction 1 and the subsequent decay reaction 2 take place, and "dark" propagation stage that does not require further photoexcitation because the self-sustainable pair of reactions 3 and 4 can proceed autocatalytically. This mechanism implies two distinct dynamic reaction regimes, the first of which corresponds to an induction period, while the second one represents self-accelerated solid-state chain reaction. The discontinuous increase of the arsenolite bands in the IR spectrum (Table 2, Figure 4) as well as of its oxygen peaks in the XPS spectrum under ultrahigh vacuum conditions[29] supports the two-regime model. Further support comes from the slow dynamics of realgar monitored with powder

(38) Farmer, V. C., Ed. *The Infrared Spectra of Minerals*; Mineralogical Society: London, 1974.
(39) Grzechnik, A. *J. Solid State Chem.* **1999**, *144*, 416−422.

Table 2. Band Frequencies and Intensities in the Far-IR Spectra of Pure Realgar and Mixtures Obtained by Exposure of Realgar to Natural Sunlight[a,b]

0 days	30 days	60 days	90 days	120 days	150 days	180 days	1000 days	trend[c]	assignment[20]
				492 vvw	*492 vvw*	*492 vvw*	*492 vvw*		arsenolite
			479 vw	*478 vw*	*478 vw*	*478 w*	*478 w*		arsenolite
			444 vw	*442 vw*	*445 vw*	*444 vvw*	*443 vw*		arsenolite
374 m	374 w	374 w	377 sh	**381 sh**	**383 w**	**383 m**	**383 m**	↑	ν(As−S)
368 m	368 m	368 m	368 w	368 vw	**367 sh**	**366 sh**	**365 vw**	↓	ν(As-S)
358 w	358 w	358 w	357 w	357 w	*356 m*	***356 m***	***356 m***	↓	ν(As-S)
341 vs	341 vs	341 s	341 m	*343 vw*	*347 w*	***348 m***	***348 m***	↑	ν(As-S)
327 sh	327 sh	327 sh	327 m	327 sh	**327 vw**	**327 w**	**327 w**	NC	ν(As-S)
				319 vw	**319 w**	**319 w**	**319 m**		
	256 sh	*256 sh*	*256 vw*	*256 w*	*256 w*	*256 m*	*256 m*	NC	arsenolite
	236 sh	236 sh	236 vw	**236 vw**	**236 w**	**236 m**	**236 m**	NC	
225 s	225 s	225 s	225 s	225 s	**225 vw**	**222 vw**	**225 vw**	NC	ω(As−S−As)
210 w	210 w	210 w	210 w	210 w	**210 vw**	**210 vw**	**210 vw**	NC	δ(As−S−As)
203 w	203 w	203 w	200 w	198 vw	**198 w**	**198 w**	**198 w**	↓	
193 w	193 w	191 w	190 w	188 m	**188 m**	**188 m**	**188 m**	↓	δ(As−S−As)
183 w	183 w	183 vw	183 vw	183 sh			**183 sh**	NC	ν(As−As)
168 m	168 m	168 m	168 m	168 m	**168 m**	**168 m**	**168 m**	NC	ω(As−S−As)
		153 vw		156 vw	**156 w**	**156 w**	**156 w**		

[a] Intensity codes: v, very; s, strong; w, weak; m, medium; sh, shoulder. The bands assignable to the intermediate χ-phase (close to β-As_4S_4), arsenolite, and pararealgar are presented as combinations of underlined, italic, and bold characters, respectively. The bands of arsenolite were assigned by comparison with the literature data[39] for the pure compound (255 s, 288 vw, 302 vw, 340 vs, 380 sh, 415 w, 442 w, 480 vs and 495 w). [b] The peak maxima were extracted from the native (nonfitted) spectra. [c] Frequency change codes: ↑, increased intensity; ↓, decreased intensity; NC, no observable change in the intensity.

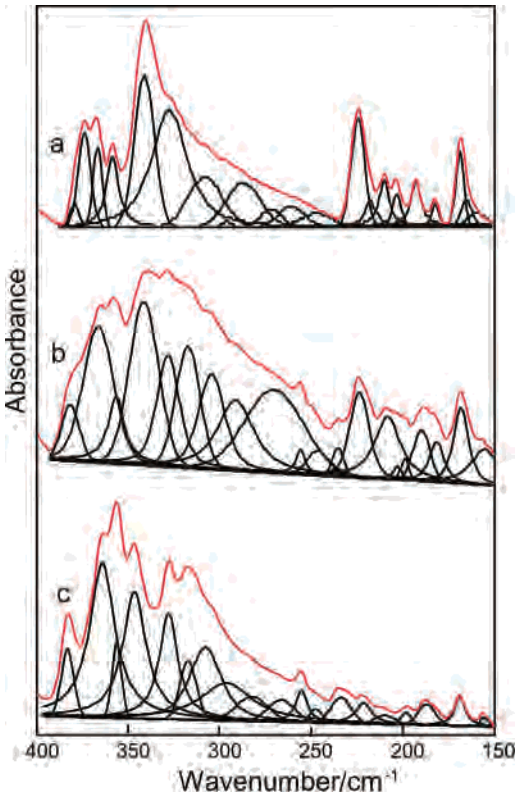

Figure 4. Results from the fitting of the far-IR spectra of realgar (a), pararealgar (c), and an intermediate mixture of phases obtained after 120 days of exposure of realgar to natural sunlight (b). All fitted spectra are deposited as Supporting Information (Figure S1).

X-ray diffraction, exhibiting two linear regimes of concentration variation of the arsenolite phase simultaneously with steady decrease of the realgar phase and increase of the pararealgar phase.[28] The ratio of the intermediate β-As_4S_4 phase follows more complex pattern, increasing to a maximum of about 30% and decreasing to zero afterward.[28] The difference between the discontinuous change of cell parameters in the case of irradiated pure realgar and the continuous change observed in the case of pure β-As_4S_4 and its mixed crystals (the lattice of the latter being more compatible with the intermediate phase) was also pointed out recently by Bonazzi et al.[31,32]

To obtain direct evidence of the reaction mechanism with atomic level resolution, the transformation at room temperature was studied with in situ single-crystal photodiffraction, by combining excitation of the sample with visible light and probing the resulting structural changes with single-crystal X-ray diffraction. Except for the different choice of the setting of the monoclinic cell (we choose $a = 6.6$ Å and $c = 9.3$ Å, so that $a < c$, while in the previous studies the opposite assignment of a and c axes was chosen),[10,29] the structures of nonirradiated crystals **A** and **B** conform to the literature data for the form α realgar.[9,10] The structure of our natural specimen from Allchar was best described in the space group $P2_1/n$. The cell parameters measured from crystal **A** are the following: $a = 6.5776(10)$, $b = 13.5341(21)$, $c = 9.3089(15)$ Å; $\beta = 106.530(2)°$; $V = 794.4(2)$ Å^3. Each of the four equivalent As_4S_4 clusters in the unit cell adopts a cradle-type conformation with $\bar{4}2m$ symmetry, which can be described as an As_4 disphenoid bisected by a S_4 square (Figure 1).[28] The relevant interatomic distances, angles, and fractional coordinates are listed in Tables 3−5. The clusters are organized in corrugated layers which interact through van der Waals forces and form ABAB type stacks (Figure 2; in form β of realgar the molecules exist in the same conformation, but they are organized in layers of AAAA stacks instead). For comparison, the crystal of pararealgar is of monoclinic $P2_1/c$ symmetry, with $a = 9.9092$, $b = 9.6551$, and $c = 8.5021$ Å and $\beta = 97.29°$.[15] Similarly to realgar, there are four As_4S_4 clusters in the unit cell held together by van der Waals forces (Figure 2). The As_4S_4 clusters of pararealgar differ from those of realgar by their topology, and the two compounds can be considered linkage isomers. In the structure of realgar, each As atom is bonded to two S atoms and to one As atom, so that the arsenic−

Table 3. Selected Intracluster Distances (Å) in the Structure of Realgar, before and after Irradiation with Visible Light (This Study), and in the Structure of Pararealgar[15]

realgar					pararealgar	
bond	cryst **A**, before	cryst **A**, after[a]	cryst **B**, before	cryst **B**, after[a]	bond	
As1−S1	2.2371(18)	2.237(3)	2.2407(13)	2.298(8)	As1−S1	2.255
As1−S2	2.2321(18)	2.228(3)	2.2321(14)	2.298(7)	As1−S3	2.239
As1−As4	2.5671(10)	2.566(2)	2.5707(8)	2.661(5)	As1−S4	2.262
As2−S1	2.2401(18)	2.235(3)	2.2440(13)	2.304(8)	As2−S1	2.252
As2−S3	2.2337(18)	2.237(3)	2.2352(13)	2.319(7)	As2−S2	2.253
As2−As3	2.5632(10)	2.559(2)	2.5644(8)	2.639(4)	As2−As4	2.484
As3−S2	2.2468(17)	2.241(3)	2.2465(13)	2.301(8)	As3−S2	2.244
As3−S4	2.2363(18)	2.233(3)	2.2354(13)	2.310(8)	As3−S3	2.228
As4−S3	2.2311(19)	2.222(3)	2.2317(14)	2.289(8)	As3−As4	2.534
As4−S4	2.2300(18)	2.228(3)	2.2304(14)	2.291(7)	As4−S4	2.191

[a] As refined without treatment of the disorder.

Table 4. Selected Intracluster Angles (deg) in the Structure of Realgar, before and after Irradiation with Visible Light (this Study), and in the Structure of Pararealgar[15]

realgar					pararealgar	
angle	cryst **A**, before	cryst **A**, after[a]	cryst **B**, before	cryst **B**, after[a]	angle	
S1−As1−S2	94.89(6)	94.85(11)	94.91(5)	94.6(3)	S1−As1−S3	103.63
As4−As1−S1	98.63(5)	98.66(8)	98.65(4)	98.9(2)	S1−As1−S4	96.23
As4−As1−S2	99.24(5)	99.13(8)	99.13(4)	98.9(2)	S3−As1−S4	98.33
S1−As2−S3	94.43(7)	94.19(11)	94.41(5)	94.7(3)	S1−As2−S2	105.53
As3−As2−S1	99.54(5)	99.58(8)	99.58(4)	99.2(2)	S1−As2−As4	100.03
As3−As2−S3	99.20(5)	99.07(9)	99.19(4)	98.8(2)	S2−As2−As4	87.03
S2−As3−S4	95.05(7)	94.93(11)	95.02(5)	95.0(3)	S2−As3−S3	103.24
As2−As3−S2	99.16(5)	99.15(8)	99.15(4)	99.3(2)	S2−As3−As4	86.03
As2−As3−S4	99.51(5)	99.40(9)	99.43(4)	98.7(2)	S3−As3−As4	100.03
S3−As4−S4	95.02(7)	94.84(11)	94.91(5)	93.8(3)	S4−As4−As2	101.72
As1−As4−S3	99.82(5)	99.65(8)	99.78(4)	99.6(2)	S4−As4−As3	101.03
As1−As4−S4	99.84(5)	99.77(8)	99.81(4)	99.6(2)	As2−As4−As3	83.41
As1−S1−As2	101.38(6)	101.44(10)	101.29(5)	101.8(3)	As1−S1−As2	109.24
As1−S2−As3	101.17(6)	101.40(10)	101.32(5)	101.8(3)	As2−S2−As3	95.94
As2−S3−As4	100.93(6)	101.23(11)	100.99(5)	101.5(3)	As1−S3−As3	110.53
As3−S4−As4	100.70(7)	100.94(11)	100.84(5)	101.6(3)	As1−S4−As4	104.44

[a] As refined without treatment of the disorder.

sulfur cluster includes eight As−S bonds and two As−As bonds (Figure 1a). In pararealgar, three As bonding patterns exist: one As atom is bonded to two As atoms and one S atom, one As atoms is bonded to three S atoms, and two As atoms are each bonded to two S atoms and one As atom (Figure 1b). The arsenic−sulfur cluster thus includes eight As−S bonds and two As−As bonds.

In the light stage of the reaction (during photoexcitation) the cell parameters of crystal **A** did not change significantly, even at increased light intensity. The cell parameters of the photoirradiated crystal are the following: $a = 6.5800(39)$, $b = 13.5288(80)$, $c = 9.3224(56)$ Å; $\beta = 106.242(9)°$ (+0.04%, −0.04%, and +0.14% for $a-c$ axes, respectively, relative to the initial values). Likewise, the cell volume remained identical, $V = 796.8(8)$ Å^3 (+0.29%). Except for slight shortening of the As4−S3 bond, the interatomic distances during irradiation are, within the experimental uncertainty, identical with the respective values before irradiation (Table 3). Although the cluster geometry remained unchanged, the 3D difference electron map of the model refined with anisotropic atomic thermal parameters exhibited new residual features, indicating increased disorder (Figure 5b). Of the several residual peaks, the highest one was at 1.0 Å from S3, while the second highest was at approximately half the distance between As1 and S1. The photoexcitation results in increased atomic motions in the crystal, but at this stage neither the geometry of the cluster nor the intercluster separation is significantly affected. This observation is probably due to the space- and time-averaging of the interatomic bond distances and cell parameters over crystal volume and data collection time, because at this stage of the reaction the majority of molecules in the crystal is in the form of realgar.

Figure 6b represents single-molecule model of the structure in the light phase, where the most intense residual peaks have been assigned to partially occupied atoms of a secondary molecular component. The accumulation of electron density in the structure during excitation relative to the crystal before excitation indicates that the reaction initiation takes place by positional offset of the cage atoms. This is most evident with the sulfur atom S3, which shifts (to S3′) around 1 Å toward S4 from its original position. Also offset are the arsenic atoms As1, As3, and As4, while S4 and As2 experience smaller displacements and in the model they are represented at their original positions. The peak appearing close to the bisector of As1 and As4 is attributed to a new atom, S5′. The topology of the secondary component, with its atoms assigned on the basis of the presumption (on the basis of discrete structures of the known arsenic sulfides in Figure 1a−d) that sulfur atoms always bridge a pair of arsenic atoms, corresponds to the topology of tetraarsenic pentasulfide, As_4S_5, where two As−As edge-sharing enve-

Table 5. Fractional Atomic Coordinates and Equivalent Isotropic Thermal Coefficients

atom	*x*	*y*	*z*	U_{eq}/Å^2
		crystal **A**, before		
As4	0.214 59(10)	0.338 99(5)	0.539 41(7)	0.022 83(19)
As2	0.356 08(10)	0.361 07(5)	0.923 67(7)	0.020 90(19)
As1	0.263 39(10)	0.520 69(4)	0.621 03(7)	0.021 30(19)
As3	0.677 75(9)	0.373 54(5)	0.820 97(7)	0.020 86(19)
S2	0.615 8(2)	0.523 61(11)	0.714 27(19)	0.023 2(4)
S4	0.552 3(3)	0.290 04(12)	0.606 68(19)	0.026 3(4)
S3	0.139 6(3)	0.273 95(12)	0.738 61(19)	0.025 2(4)
S1	0.200 9(2)	0.506 19(12)	0.844 07(19)	0.023 9(4)
		crystal **A**, after		
As2	0.355 64(17)	0.360 86(7)	0.923 92(12)	0.027 7(3)
As4	0.214 68(17)	0.339 24(7)	0.540 37(12)	0.031 3(3)
As1	0.264 12(17)	0.520 75(7)	0.622 67(12)	0.029 1(3)
As3	0.676 63(16)	0.373 20(7)	0.820 80(12)	0.027 8(3)
S1	0.201 5(4)	0.505 86(18)	0.845 5(3)	0.031 2(6)
S4	0.551 1(4)	0.289 95(19)	0.607 4(3)	0.035 0(7)
S2	0.615 1(4)	0.522 92(18)	0.714 5(3)	0.030 8(6)
S3	0.139 2(4)	0.274 52(18)	0.738 5(3)	0.033 7(6)
		crystal **B**, before		
As4	0.714 56(8)	0.339 01(4)	0.039 45(5)	0.028 22(15)
As2	0.856 25(8)	0.361 04(3)	0.423 72(5)	0.026 27(15)
As1	0.763 40(8)	0.520 74(3)	0.121 14(5)	0.026 61(15)
As3	1.177 83(7)	0.373 52(4)	0.320 92(6)	0.026 15(15)
S4	1.052 1(2)	0.290 09(9)	0.107 04(14)	0.031 9(3)
S2	1.115 57(19)	0.523 32(8)	0.214 13(14)	0.027 8(3)
S3	0.639 6(2)	0.274 12(9)	0.238 64(14)	0.030 5(3)
S1	0.700 81(19)	0.506 25(9)	0.344 38(14)	0.028 9(3)
		crystal **B**, after[a,b]		
As1	−0.234 47	0.521 38	0.126 04	
As3	0.174 64	0.372 51	0.319 20	
S2	0.114 75	0.521 78	0.215 28	
S3	−0.361 45	0.274 37	0.238 52	
As1′	−0.077 55	0.536 78	0.197 33	
AS3′	0.126 68	0.395 25	0.328 92	
S2′	−0.277 70	0.482 27	0.024 67	
S3′	−0.244 45	0.265 98	0.212 51	
As2	−0.147 84	0.360 68	0.423 18	
As4	−0.285 39	0.339 84	0.041 89	
S1	−0.297 40	0.506 24	0.346 65	
S4	0.047 38	0.289 67	0.108 81	

[a] As refined with treatment of the disorder. [b] The displacement parameters were subjected to restraints.

lopes are connected by an S atom (Figure 1d). The structure of the crystal in the light phase, therefore, can be considered an evidence of accumulation of As_4S_5 cages in the lattice, where the overall crystalline disorder has been preserved.

In the light stage of the reaction, the crystal is able to sustain the stress induced by evolution of the secondary As_4S_5 lattice, so that the overall crystalline order and the gross unit cell are retained. As it was shown[32] recently with the case of β-As_4S_4 (which undergoes continuous photoinduced transformation), increased population of As_4S_5 cages to measurable amounts is expected to result in significant expansion of the cell. Because the concentration of As_4S_5 cages in the irradiated crystal of realgar is very small and the irradiation time is very short (1.3 h), the lattice parameters remain nearly constant. Although the changes of cell parameters are very small, taking into account the different choice of the cell, they are still in agreement with the lattice changes observed by Bonazzi et al.[27] on prolonged irradiation. This result confirms the suggestions[32] that contrary to β-As_4S_4, whose molecular packing allows very large portion of As_4S_4 cages to be substituted with As_4S_5 cages and thus

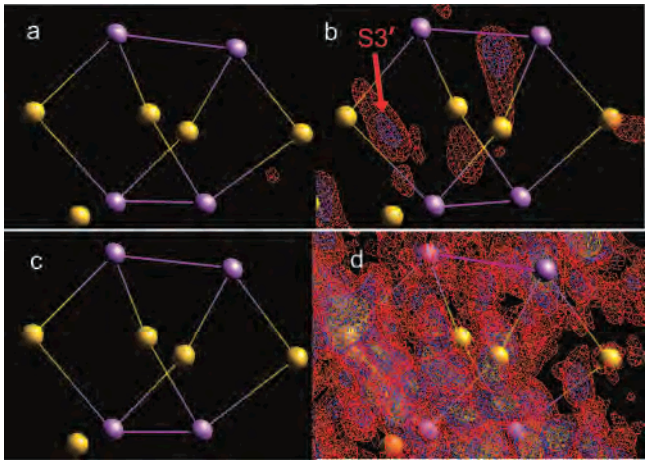

Figure 5. Changes of the 3D difference ($F_o - F_c$) Fourier maps of realgar in the light phase (b, during photoirradiation, crystal **A**) and in the dark phase (d, after photoirradiation, crystal **B**). (a) and (c) represent the respective maps before irradiation. The red, blue, and yellow isosurfaces correspond to electron density surplus of 1.0, 1.5, and 2.0 e·Å^{-3}, respectively. The arsenic and sulfur atoms are represented as magenta and beige circles, respectively.

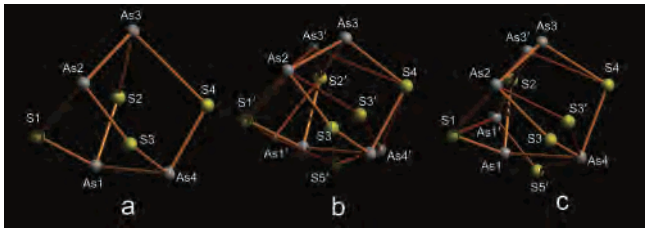

Figure 6. Structure and topology of the As_4S_4 cluster of realgar before (a), during (b), and after (c) irradiation with visible light. The structures in (a) and (b) are refined as anisotropic single-molecule models; the structure in (c) is refined as a mixed two-molecule model. The peaks assigned to the photoinduced components are denoted with primed labels, and the respective bonds are shown in brown color. Arsenic and sulfur atoms are represented as gray and yellow circles, respectively.

undergoes a continuous light-induced process, in the case of realgar only small amount of the molecules can be substituted. This is only possible in the initial stages of the transformation. The inability of the molecular packing of realgar to accommodate larger number of As_4S_5 cages results in a discontinuity of the process and strong cell expansion in the later stages (see below).

In the case of crystal **B** before excitation, the highest difference peak in the 3D Fourier map of the anisotropic model was only 0.6 e·Å^{-3}. At room temperature, the cell parameters were $a = 6.5809(10)$, $b = 13.5512(21)$, and $c = 9.3169(14)$ Å and $\beta = 106.505(2)°$, and the structure was identical with that of crystal **A** before irradiation. Initial exposure of the red crystal **B** to visible light and subsequent immediate data collection in the dark (∼13 h) resulted in drastic changes in reflection intensities, and the crystal gradually turned orange-yellow and opaque. As a result of the pronounced expansion along the $a-c$ axes of 3.30%, 3.25%, and 3.79%, respectively, to $a = 6.798(5)$, $b = 13.991(11)$, and $c = 9.673(7)$ Å and $\beta = 105.419(13)°$, the unit cell underwent strong but nearly isotropic expansion and its volume increased 90 Å^3 (11.3%), from 796.6(2) to 886.9(11) Å.^{3} The strong cell expansion was reflected in notable stretching of all intracluster atom−atom bonds (Table 3) and

increased intercluster distances. Therefore, our results suggest that the expansion appears as joint result of expansion of the As_4S_4 clusters *and* increased separation of the clusters in the cell. It should be noted that the volume expansion in our study (90 $Å^3$) is much larger than the values ($\sim$10 $Å^3$) reported previously,[27,29] which may be due to the different experimental conditions of photoexcitation. The strong expansion of the cell observed in our experiment reflects the elongation of the interatomic distances when the disorder has not been treated (Table 3). Even without fitting into a two-component model, these values show that not only the intermolecular separation but also the average interatomic distances between As and S atoms increased after irradiation. The effect on the average distances is a collective result of the bond stretching and the lattice superposition of the reactant realgar and product molecules. Namely, although the amount of the secondary component in the crystal is small, the mismatch of size and orientation of the two lattices and the different positions of the atoms from the two components appear as bonds which are longer than those of realgar but are still within the range of normal As−S distances. The light-induced changes of the intercage separation, however, are insufficient to consider formation of intermolecular bonds.

As shown in Figure 5d, refinement of the structure after irradiation as anisotropic model shows significantly high residual electron density, the largest peak (>2 e·$Å^{-3}$) being at 1.1 Å from S3. In addition to the positional shift of S3, there is significant offset of the atoms As1 and As3 from their original positions. In the structure refined as a model composed of two molecules with complementary occupancies, each of these three atoms (S3, As1, and As3) was split into two components. In the minor photoinduced component, As1′ and As3′ are closer to each other relative to their major counterparts As1 and As3, and with As2 they form the triangular As_3 substructure characteristic for the cluster of pararealgar (Figure 1b). The peak close to the bisector of the As1−As4 bond is assigned to a new sulfur atom S5′, bridging As1′ and As4. The atom topology of the secondary structure, whose occupancy refined to 5%, corresponds to that of pararealgar. Therefore, the crystal in the dark stage represents a photochemically produced mixture composed of 95% realgar and 5% pararealgar. Comparison of the nonexcited and photoinduced structures (Figure 6a,c) shows that the atom S2, bridging As1 and As3, was detached from the molecule, while S5′ was attached between As1 and As4. In effect, S2 and As1 have switched their positions, and S2 has become S5′. Unfortunately, it was not possible to obtain a higher concentration of the pararealgar form in the single crystal, due to the significantly increased mosaicity after prolonged storage of the sample. This observation is consistent with the crystal degradation observed in the previous studies.[29] The loss of long-range crystalline order and decreased crystal quality are probably due to the large structural rearrangements related to incompatibility of the evolving pararealgar lattice with the host realgar lattice.[32]

The extra sulfur atom S5′ is inserted in the bond As1−As4. The preference of this bond over As2−As3 may be due to several reasons, including differences in partial charges of the As atoms or different intermolecular orientation of the two bonds. As1−As4 is only marginally longer than As2−As3 (Table 3), so that bond length cannot be considered as an indicator for the preferred reactivity. In both the light and dark reaction stages, atom S3′ had larger population than the other atoms of the product pararealgar cluster, and it seems a probable initiation point of the photoreaction. Compared to the other As−S bonds (Table 3), As2−S3 and As4−S3 are not extremely long. Therefore, the reactivity of the As2−S3−As4 bridge is probably due to balanced strength of the two bonds rather then to their length: the As−S bond length difference (0.0026 Å) is similar or smaller than those of the other three bridges (0.0030, 0.0063, and 0.0147 Å).

Comparison of cluster structures of realgar and pararealgar (Figure 1a,b) shows that they have in common half of the molecule letter-type conformer of the As_2SAsS moiety, while the other half differs by the topology of two atoms: one As and one S atom in the cluster of pararealgar have their positions exchanged. In the structure of the intermediate phase As_4S_5 (Figure 6b), the As2−As3 bond is preserved (as As2−As3′), whereas As1−As4 is broken by insertion of the sulfur atom S5′. The former continues to exist in the dark stage of the process, and it is also preserved in the structure of pararealgar (Figure 6c). Transformation of the intermediate As_4S_5 to pararealgar proceeds by dissociation of one sulfur atom (S2) and rebonding of the rest of the molecule, with the new sulfur atom (S5′) taking the position of one of the As atoms (As1), which in turn (As1′) has replaced the leaving sulfur atom (S2). This means that the fragment As2As3S4As4S3 is the half-molecule fragment which survives the transformation of realgar to pararealgar as As2As3′S4As4S3′ (Figure 6c).

Solely on the basis of our present results, it is not possible to address entirely the issue of whether the photoinduced transformation of realgar is intermolecular or intramolecular process. Although the bond distances in the two points probed here imply an intramolecular process, this hypothesis needs to be supported with a step-by-step structural analysis at several points of the transformation, which would afford the time-dependent changes of atom populations. We believe that this point could become a basis for a further in-depth structural study of the light-induced transformation of realgar.

Acknowledgment. We cordially thank the anonymous reviewers for the constructive comments and suggestions. This study was performed through the Special Coordination Funds for Promoting Science and Technology from the MEXT of the Japanese Government and was financially supported by the Ministry of Education and Science of the Republic of Macedonia.

Supporting Information Available: Plots of all fitted spectra (Figure S1) and a table with frequencies and intensities of the fitted IR spectra (Table S1). This material is available free of charge via the Internet at http://pubs.acs.org.

IC701299W